

A Chromium(II) Tetracarbene Complex Allows Unprecedented Oxidative Group Transfer

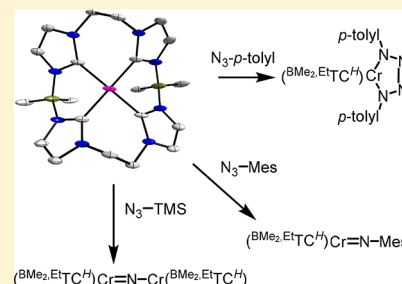
Gaya R. Elpitiya,[†] Brian J. Malbrecht,[‡] and David M. Jenkins^{*,†}

[†]Department of Chemistry, University of Tennessee, Knoxville, Tennessee 37996, United States

[‡]Department of Chemistry and Chemical Biology, Harvard University, Cambridge, Massachusetts 02138, United States

Supporting Information

ABSTRACT: Multiple distinct oxidative group transfer reactions to low valent chromium were examined. Six new chromium complexes were prepared from a highly electronically unsaturated Cr(II) square planar complex that was supported by a macrocyclic tetracarbene ligand. This complex's reactivity with Me₃NO and disparate azides was investigated. The reaction with Me₃NO generated a highly stable Cr(IV)-oxo complex. Less bulky organic azides such as *p*-tolyl and *n*-octyl azides gave rise to metallotetrazenes, while more sterically demanding mesityl and adamantyl azides generated Cr(IV)-imido complexes. The reaction of the square planar Cr(II) complex with TMS-azide yielded the first linearly bridging nitrido chromium species. Reductive group transfer was explored for a Cr(IV)-imido complex, and organic products, such as aziridines, were formed after addition. Cr(IV) imidos and oxos are quite rare, while tetrazenes and bridging nitridos are virtually unknown. This is the most detailed study on oxidative group transfer reactions using chromium based complexes on a single auxiliary ligand to date.



INTRODUCTION

The exploration of new metal–ligand multiple bonds on earth abundant transition metals continues to be an active area of research in inorganic chemistry due to their importance as intermediates in oxidative group transfer reactions, ranging from alkane hydroxylation^{1–7} to aziridination.^{8–13} For example, biomimetic iron-oxo complexes have been scrutinized extensively due to their ability to mimic oxidative reactions that occur in both cytochrome P450 and nonheme enzymes.^{3,6,7,14,15} Recent iron oxo and imido complexes have demonstrated remarkable reactivity including novel routes for C–H bond functionalization.^{12,16,17} In each of these cases, the key iron–ligand multiple bond is formed through an oxidative group transfer reaction. Despite widespread fresh investigations of oxidative group transfer on iron complexes in the past decade, few recent studies have been reported on early transition metals such as chromium.^{17–20}

While chromium oxo and imido complexes have been synthesized via oxidative group transfer, they are almost all high valent Cr(V) and Cr(VI) complexes supported with auxiliary ligands such as porphyrins, phthalocyanins, salens, or β -diketiminates.^{21–28} Furthermore, these high valent chromium complexes often showed limited reactivity for reductive transfer of the oxo or imido.^{20,21,26,29–32} While lower valent chromium complexes may have more facile group transfer of an imido^{33–39} or oxo,^{40–44} only a very limited number of these complexes have been synthesized (Figure 1).

One tactic to improve group transfer on chromium complexes is to switch to stronger σ -donating auxiliary ligands, which have proven very successful in developing novel oxidative group transfer reactions on iron.^{45–51} Macrocyclic N-

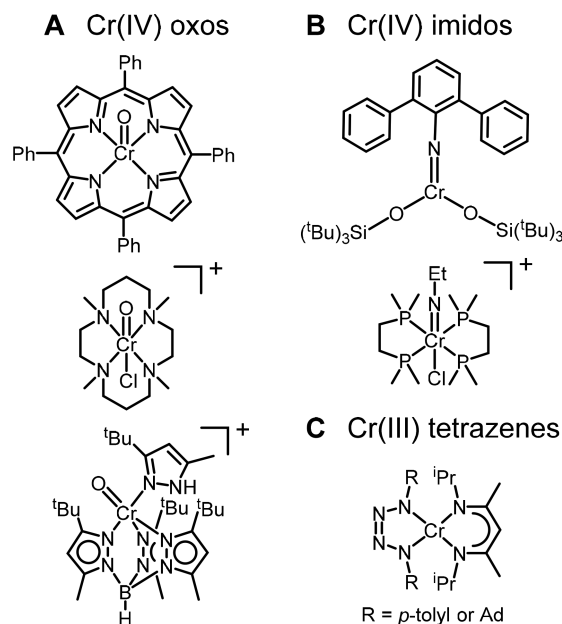


Figure 1. Selected examples of the limited midvalent Cr(IV) oxos (A), Cr(IV) imidos (B), and Cr(III) tetrazenes (C) that were previously reported.

heterocyclic carbenes (NHCs) are strong σ -donor ligands that are structurally similar to, but electronically distinct from, other macrocyclic ligands, such as porphyrins, that have been

Received: September 1, 2017

studied extensively on chromium.^{40,42} Macrocyclic NHCs have proven versatile for probing group transfer on iron as both iron(IV) oxos and iron(IV) tetrazenes have been synthesized.^{10,52–54} Furthermore, macrocyclic NHC iron complexes are quite effective for supporting catalytic group transfer reactions, particularly aziridination.^{9–11} Despite their potential application for oxidative group transfer on chromium, only one chromium tetra-NHC complex has been reported previously.⁵⁵

In this paper, we assess whether midvalent chromium(IV) imidos and oxos are viable for group transfer reactions in a manner similar to that for iron(IV), by showcasing a comprehensive survey of chromium(IV) complexes with distinct metal–ligand multiple bonds supported by a single auxiliary ligand. This begins with the synthesis of an electronically unsaturated square planar Cr(II) complex with our second generation NHC-borate macrocycle.⁵⁶ This Cr(II) complex is highly reactive toward group transfer oxidants such as organic azides and Me₃NO. Sterically bulky azides, such as adamantyl azide, lead to the formation of rare Cr(IV) imido complexes. Less encumbered organic azides, such as octyl azide, lead to metallotetrazene complexes that are formed in a formal [2 + 3] cycloaddition reaction from the metal-imido intermediate. These metallotetrazenes are the first examples of Cr(IV) tetrazenes. Notably, the reaction of the Cr(II) complex with TMS-N₃ gives the first isolable Cr(III/IV) μ -nitrido species. In addition to the oxidative group transfer, the reactivities of the Cr(IV) imido and oxo species were tested for reductive group transfer. While the chromium oxo complex showed no release of the oxo ligand, the chromium imido complex showed excellent reactivity toward group transfer to decene and triphenyl phosphine, yielding the aziridine and phosphanimine, respectively. This broad selection of complexes and reactions with azides makes this macrocyclic NHC system the most versatile and widely characterized system for oxidative group transfer reactions on chromium to date.

EXPERIMENTAL SECTION

General Methods and Procedures. All reactions were performed under a dry nitrogen atmosphere with the use of either a drybox or standard Schlenk techniques. Solvents were dried on an Innovative Technologies (Newburgport, MA) Pure Solv MD-7 Solvent Purification System and degassed by three freeze–pump–thaw cycles on a Schlenk line to remove O₂ prior to use. Benzene-*d*₆ and chloroform-*d* were degassed by three freeze–pump–thaw cycles prior to drying over activated molecular sieves. These NMR solvents were then stored under N₂ in a glovebox. The compounds *n*-octyl azide, *p*-tolyl azide, mesityl azide, and (BMe₂EtTC^H)(Br)₂ (**1**)⁵⁶ were prepared from literature procedures. All other reagents were purchased from commercial vendors and used without purification. ¹H, ¹³C{¹H}, and ³¹P NMR spectra were recorded at ambient temperature on a Varian VNMRs 500 MHz narrow-bore broadband system. ¹H and ¹³C NMR chemical shifts were referenced to the residual solvent. All mass spectrometry analyses were conducted at the Mass Spectrometry Center located in the Department of Chemistry at the University of Tennessee. The DART analyses were performed using a JEOL AccuTOF-D time-of-flight (TOF) mass spectrometer with a DART (direct analysis in real time) ionization source from JEOL USA, Inc. (Peabody, MA). Mass spectrometry sample solutions of metal complexes were prepared in tetrahydrofuran. Mass spectrometry sample solutions of organic compounds were prepared in ethyl acetate. Infrared spectra were collected on a Thermo Scientific Nicolet iS10 with a Smart iTR accessory for attenuated total reflectance. UV–vis measurements were taken inside a dry glovebox on an Ocean Optics USB4000 UV–vis system with 1 cm path length quartz crystal cell. Room temperature magnetic measurements using Evans NMR were not successful due to poor solubility of the complexes in common

deuterated solvents. Despite multiple attempts, extreme sensitivity of the complexes led to elemental analyses that were outside the range viewed as establishing analytical purity. Elemental composition was confirmed by high resolution mass spectrometry.

Synthesis and Characterization of Chromium Complexes. [(BMe₂EtTC^H)Cr], **2**. (BMe₂EtTC^H)(Br)₂ (**1**) (0.300 g, 0.530 mmol) was added to tetrahydrofuran (40 mL) in a 100 mL round-bottom flask and stirred for 10 min. *n*-BuLi (0.586 g, 2.11 mmol) was pipetted into the stirring (BMe₂EtTC^H)(Br)₂ mixture. After 20 min, chromium(II) chloride (0.065 g, 0.53 mmol) was added to the reaction mixture. The reaction mixture was allowed to stir for 18 h at room temperature. The slurry was filtered over Celite to collect the filtrate. All volatiles were removed under reduced pressure. Benzene (50 mL) was added to the crude solid in 10 mL portions, and the product was extracted as yellow solution. The yellow solution was then filtered, and the collected filtrate was concentrated to 10 mL. The pure product was crystallized via vapor diffusion of pentane into the benzene solution, and the bright yellow crystals were collected in two batches (0.144 g, 60.0% yield). ¹H NMR (benzene-*d*₆, 499.74 MHz): δ -1.44, -30.59. UV–vis (THF) λ_{max} nm (ϵ): 419 (320). DART HR MS (*m/z*): [M]⁺ 454.20156 (found), 454.20282 (calcd).

[(BMe₂EtTC^H)Cr(O)], **3**. This was synthesized by two methods. Method 1 follows: [(BMe₂EtTC^H)Cr] (**2**) (0.100 g, 0.219 mmol) was added to tetrahydrofuran (10 mL) in a 20 mL vial and stirred for 5 min. Me₃NO (0.019 g, 0.25 mmol) was added in to the stirring solution of **2**. The reaction mixture was allowed to stir for 48 h at room temperature. The slurry was filtered over Celite to collect the filtrate. All volatiles were removed under reduced pressure. Benzene (20 mL) was added to the crude solid in 10 mL portions, and the product was extracted as green solution. The green solution was then filtered, and the collected filtrate was concentrated to 5 mL. The pure product was crystallized via vapor diffusion of pentane into the benzene solution, and the bright green crystals were collected (0.0140 g, 14.0% yield). Method 2 follows: [(BMe₂EtTC^H)Cr] (**2**) (0.100 g, 0.219 mmol) was added to tetrahydrofuran (10 mL) in a 50 mL Schlenk flask inside the glovebox. The flask was thoroughly greased and sealed and was brought out of the glovebox and connected to a flow of N₂ under Schlenk line. A 2.7 mL (0.011 mmol) portion of dry O₂ was syringed carefully into the mixture of **2** in tetrahydrofuran and stirred for 5 min. The reaction mixture turned from bright yellow to green immediately, and all volatiles were removed under reduced pressure after 5 min. The reaction flask was brought into the glovebox, and the green compound was extracted with benzene (20 mL) and was filtered through Celite. The bright green crystals were obtained in the same way as in Method 1. (0.052 g, 50% yield). ¹H NMR (benzene-*d*₆, 499.74 MHz): δ -1.39. IR: 2929, 1587, 1444, 1412, 1285, 1204, 1147, 1113, 1031 (Cr=O), 942, 788, 734, 678 cm⁻¹. UV–vis (THF) λ_{max} nm (ϵ): 483 (140), 627 (40). DART HR MS (*m/z*): [M + H]⁺ 471.20696 (found), 471.20501 (calcd).

[(BMe₂EtTC^H)Cr(*p*-tolyl)N₄(*p*-tolyl)], **4**. [(BMe₂EtTC^H)Cr] (**2**) (0.100 g, 0.219 mmol) was added to tetrahydrofuran (10 mL) in a 20 mL vial and stirred for 5 min. *p*-Tolylazide (0.087 g, 0.66 mmol) was added to the stirring solution of **2**. The reaction mixture was allowed to stir for 24 h at room temperature. The slurry was filtered to collect the filtrate. All volatiles were removed under reduced pressure. Benzene (30 mL) was added to the crude solid in 10 mL portions, and the product was extracted as deep red solution. The deep red solution was then filtered, and the collected filtrate was concentrated to 10 mL. The pure product was crystallized via vapor diffusion of pentane into the benzene solution, and the deep red crystals were collected (0.038 g, 40.0% yield). ¹H NMR (benzene-*d*₆, 499.74 MHz): δ 91.79, 48.00, 26.67, -1.20, -2.31, -10.30, -18.90, -82.75. UV–vis (THF) λ_{max} nm (ϵ): 544 (690). IR: 2925, 1500, 1422, 1284, 1196, 1148, 1111, 1034, 977, 957, 943, 821, 752, 736, 722, 703, 681 cm⁻¹. DART HR MS (*m/z*): [M + H]⁺ 693.33474 (found), 693.33194 (calcd).

[(BMe₂EtTC^H)Cr(NMes)], **5**. [(BMe₂EtTC^H)Cr] (**2**) (0.100 g, 0.219 mmol) was added to tetrahydrofuran (10 mL) in a 20 mL vial and stirred for 5 min. Mesityl azide (0.035 g, 0.22 mmol) was added in to the stirring solution of **2**. The reaction mixture was allowed to stir for 24 h at room temperature. The slurry was filtered over Celite to collect

the filtrate. All volatiles were removed under reduced pressure. Benzene (20 mL) was added to the crude solid in 10 mL portions, and the product was extracted as orange solution. The orange solution was then filtered, and the collected filtrate was concentrated to 5 mL. The pure product was crystallized via vapor diffusion of pentane into the benzene solution, and the orange crystals were collected (0.064 g, 50.0% yield). ^1H NMR (benzene- d_6 , 499.74 MHz): δ 50.65, 35.73, 9.96, -1.77, -16.78, -27.98, -46.35, -71.64. UV-vis (THF) λ_{max} nm (ϵ): 479 (800). IR: 2929, 1459, 1414, 1397, 1283, 1202, 1149, 1111, 1065, 1043, 955, 942, 852, 797, 722, 698, 680 cm^{-1} . DART HR MS (m/z): $[\text{M} + \text{H}]^+$ 588.30150 (found), 588.29924 (calcd).

$[(^{\text{BMe}_2\text{EtTC}^{\text{H}}})\text{Cr}(\text{n-octyl})\text{N}_4(\text{n-octyl})]$, **6**. $[(^{\text{BMe}_2\text{EtTC}^{\text{H}}})\text{Cr}]$ (**2**) (0.098 g, 0.22 mmol) was added to tetrahydrofuran (10 mL) in a 20 mL vial and stirred for 5 min. *n*-Octylazide (0.067 g, 0.43 mmol) was added to the stirring solution of **2**. The reaction mixture was allowed to stir for 24 h at room temperature. The slurry was filtered over Celite to collect the filtrate. All volatiles were removed under reduced pressure. Benzene (30 mL) was added to the crude solid in 10 mL portions, and the product was extracted as brown solution. The brown solution was then filtered, and the collected filtrate was concentrated to 10 mL. The pure product was crystallized via vapor diffusion of pentane into the benzene solution, and the brown-yellow crystals were collected (0.063 g, 40% yield). ^1H NMR (benzene- d_6 , 499.74 MHz): δ 16.22, 12.35, -1.84, -17.89. UV-vis (THF) λ_{max} nm (ϵ): 467 (850). IR: 2951, 2923, 2853, 1464, 1422, 1398, 1287, 1199, 1109, 1076, 1061, 1030, 958, 943, 726, 702, 685, 672 cm^{-1} . DART HR MS (m/z): $[\text{M} + \text{H}]^+$ 737.48628 (found), 737.48844 (calcd).

$[(^{\text{BMe}_2\text{EtTC}^{\text{H}}})\text{Cr}(\text{NAd})]$, **7**. $[(^{\text{BMe}_2\text{EtTC}^{\text{H}}})\text{Cr}]$ (**2**) (0.100 g, 0.219 mmol) was added to tetrahydrofuran (10 mL) in a 20 mL vial and stirred for 5 min. Adamantyl azide (0.039 g, 0.22 mmol) was added to the stirring solution of **2**. The reaction mixture was allowed to stir for 24 h at room temperature. The slurry was filtered over Celite to collect the filtrate. All volatiles were removed under reduced pressure. Benzene (20 mL) was added to the crude solid in 10 mL portions, and the product was extracted as orange solution. The orange solution was then filtered, and the collected filtrate was concentrated to 5 mL. The pure product was crystallized via vapor diffusion of pentane into a benzene and tetrahydrofuran solution mix, and the bright orange crystals were collected (0.026 g, 20% yield). ^1H NMR (benzene- d_6 , 499.74 MHz): δ 37.68, 25.60, 10.68, -1.39, 1.86, -7.85, -18.55. UV-vis (THF) λ_{max} nm (ϵ): 409 (370). IR: 2924, 2896, 1451, 1401, 1294, 1281, 1204, 1146, 1111, 1058, 1028, 1035, 945, 731, 721, 705, 677 cm^{-1} . DART HR MS (m/z): $[\text{M} + \text{H}]^+$ 604.32997 (found), 604.33054 (calcd).

$[(^{\text{BMe}_2\text{EtTC}^{\text{H}}})\text{Cr}]_2(\text{N})$, **8**. $[(^{\text{BMe}_2\text{EtTC}^{\text{H}}})\text{Cr}]$ (**2**) (0.100 g, 0.219 mmol) was added to tetrahydrofuran (10 mL) in a 20 mL vial and stirred for 5 min. Trimethylsilylazide (0.038 g, 0.3285 mmol) was added to the stirring solution of **2**. The reaction mixture was allowed to stir for 24 h at room temperature. The slurry was filtered over Celite to collect the filtrate. All volatiles were removed under reduced pressure. Benzene (30 mL) was added to the crude solid in 10 mL portions, and the product was extracted as brown solution. The brown solution was then filtered, and the collected filtrate was concentrated to 10 mL. The pure product was crystallized via vapor diffusion of pentane into the benzene solution, and the red crystals were collected (0.100 g, 50.0% yield). ^1H NMR (benzene- d_6 , 499.74 MHz): δ -1.44, -22.26. UV-vis (THF) λ_{max} nm (ϵ): 419 (570), 555 (320). IR: 2927, 1448, 1417, 1399, 1292, 1209, 1152, 1112, 1064, 1044, 942, 794, 727, 697, 672 cm^{-1} . DART HR MS (m/z): $[\text{M} + \text{H}]^+$ for the fragment $[(^{\text{BMe}_2\text{EtTC}^{\text{H}}})\text{Cr}]\text{N}$ 469.21496 (found), 469.21207 (calcd).

Group Transfer Reactions of $[(^{\text{BMe}_2\text{EtTC}^{\text{H}}})\text{Cr}(\text{NMes})]$, **5.** *Synthesis of 1-(Mesityl)-2-octylaziridine*, **9**. $[(^{\text{BMe}_2\text{EtTC}^{\text{H}}})\text{Cr}(\text{NMes})]$ (**4**) (0.050 g, 0.085 mmol) was added to a solution of 1-decene (0.012 g, 0.085 mmol) in deuterated benzene and stirred at 75 °C for 18 h. Purification by column chromatography through gradient elution (ethyl acetate/hexane) yielded the product as a yellow oil (0.020 g, 86.0%). ^1H NMR (CDCl_3 , 499.74 MHz): δ 6.75 (s, 2H), 2.31 (s, 6H), 2.21 (s, 3H), 2.10 (m, 1H), 1.49 (d, $J = 7.4$ Hz), 1.29 (m, 12H), 0.90 (t, $J = 6.8$ Hz, 3H). ^{13}C NMR (CDCl_3 , 125.66 MHz): δ 149.01, 130.85, 129.69, 129.08, 41.29, 37.04, 32.85, 32.02, 29.73, 29.71, 29.42,

26.73, 22.82, 20.56, 19.25, 14.25. DART HR MS (m/z): $[\text{M} + \text{H}]^+$ 274.25423 (found); $[\text{C}_{19}\text{H}_{32}\text{N}]^+$ 274.25293 (calcd).

Synthesis of N-Mesityl-1,1,1-triphenylphosphanimine, **10**. $[(^{\text{BMe}_2\text{EtTC}^{\text{H}}})\text{Cr}(\text{NMes})]$ (**4**) (0.021 g, 0.035 mmol) was added to a solution of triphenylphosphine (0.009 g, 0.035 mmol) in deuterated benzene and stirred at 75 °C for 48 h. Purification by column chromatography through gradient elution (ethyl acetate/hexane) yielded the product as a white crystalline solid (0.014 g, 65%). ^1H NMR (C_6D_6 , 499.74 MHz): δ 7.70–7.04 (m, 15H), 1.41–1.22 (m, 14H), 0.95 (s, 9H), 0.86 (t, $J = 7.0$ Hz, 3H). ^{31}P NMR (CDCl_3 , 125.66 MHz): δ -13.86. DART HR MS (m/z): $[\text{M}]^+$ 395.18120 (found); $[\text{C}_{27}\text{H}_{26}\text{NP}]^+$ 395.18029 (calcd).

X-ray Structure Determinations. X-ray diffraction measurements were performed on single crystals coated with Paratone oil and mounted on glass fibers. Each crystal was frozen under a stream of N_2 while data were collected on a Bruker APEX diffractometer. A matrix scan using at least 12 centered reflections was used to determine initial lattice parameters. Reflections were merged and corrected for Lorentz and polarization effects, scan speed, and background using SAINT 4.05.⁵⁷ Absorption corrections, including odd and even ordered spherical harmonics, were performed using SADABS.⁵⁸ Space group assignments were based upon systematic absences, E statistics, and successful refinement of the structure. The structures were solved by a combination of direct and intrinsic phasing method and were refined using the SHELXTL 5.0⁵⁹ software package and Olex2⁶⁰ software package. All of the non-hydrogen atoms were refined anisotropically. Hydrogen atoms attached to the carbons and nitrogens were fixed at calculated positions and refined using a standard riding model. Compounds **3**, **5**, and **8** had solvent molecule benzene cocrystallized in the asymmetric unit cell, while compound **7** had solvent molecule tetrahydrofuran cocrystallized in the asymmetric unit cell. Compounds **2** and **8** were symmetry grown, and compound **4** had two independent molecules in the asymmetric unit cell. Crystal data, data collection parameters, and results of the analyses are listed in the [Supporting Information](#).

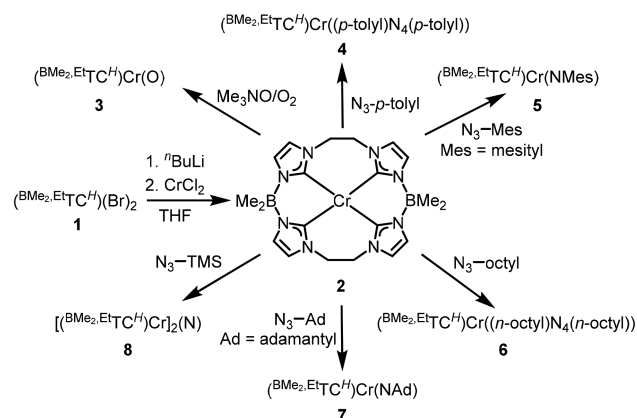
Collection of Magnetic Data. Magnetic data were collected using a Quantum Design MPMS SQUID magnetometer. Measurements were obtained for finely ground microcrystalline powders restrained in a solid eicosane matrix with gelatin capsules. Samples were prepared under a dry nitrogen atmosphere by loading the ground powder into a capsule and then adding warm liquid eicosane. The resulting mixture was agitated until homogeneous and then allowed to cool to form a solid suspension. The capsule was then immobilized in a plastic straw and mounted in the magnetometer. Direct current susceptibility measurements were collected in the temperature range 5–300 K under an applied dc field of 1 T. The susceptibility data were corrected for contributions from the sample holder and eicosane, as well as the core diamagnetism of the sample using Pascal's constants.⁶¹

Fitting of Magnetic Data. The data for **8** was fit using PHI.⁶² The $\chi_{\text{M}}T$ versus T data were fit according to an isotropic exchange coupled model with $S_1 = 1$, $S_2 = 1/2$, and $\hat{H}_{\text{ex}} = -2J\hat{S}_1\hat{S}_2$. The isotropic g values for each chromium center were constrained to be equivalent.

RESULTS AND DISCUSSION

While a previous macrocyclic chromium tetracarbene ($[(^{\text{Me}_2\text{EtTC}^{\text{H}}})\text{CrCl}_2]\text{PF}_6$) could be prepared by silver transmetalation,⁵⁵ the second generation macrocycle,⁵⁶ $(^{\text{BMe}_2\text{EtTC}^{\text{H}}})\text{(Br)}_2$ (**1**), required a direct deprotonation approach to synthesize a chromium complex (Scheme 1). Compound **1** was successfully deprotonated with $^n\text{BuLi}$ at room temperature in THF within 20 min. The addition of anhydrous CrCl_2 to the above reaction solution yielded $[(^{\text{BMe}_2\text{EtTC}^{\text{H}}})\text{Cr}]$ (**2**) in 60% yield after crystallization from a mixture of benzene and pentane. Complex **2** is a highly electronically unsaturated square planar complex, and it is extremely sensitive to both oxygen and water. The ^1H NMR of this yellow complex confirmed its paramagnetism, as expected for a Cr(II) complex. Collection of magnetic susceptibility data

Scheme 1. Synthesis of Cr(II) Complex from Macrocyclic NHC Precursor and Its Reactions with a Variety of Group Transfer Oxidants



for **2** was complicated by its extreme air-sensitivity leading to inconclusive results over multiple attempts. All of the previously reported square planar Cr(II) complexes with d^4 configuration had an $S = 2$ spin state.^{63–65} There is only one example of a Cr(II) complex with an $S = 1$ spin state but with a square pyramidal geometry.⁶⁴

Single crystal X-ray diffraction demonstrated that **2** is a square planar complex (Figure 2). The Cr–C bond distances in

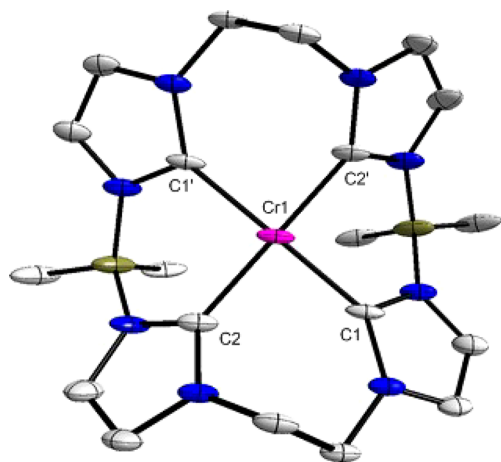


Figure 2. X-ray crystal structure of $[(\text{BMe}_2\text{EtTC}^H)\text{Cr}]$, **2**. Purple, blue, gray, and olive ellipsoids (50% probability) represent Cr, N, C, and B atoms, respectively. Solvent molecules and H atoms are omitted for clarity. Selected interatomic bond distances (Å) and angles (deg) are as follows: Cr1–C1 = 2.076(3); Cr1–C2 = 2.132(3); C1–Cr1–C1' = 170.54(14); C2–Cr1–C2' = 177.39(12).

complex **2** range from 2.076(3) to 2.132(3) Å which is within the expected range (2.08–2.18 Å) given the limited number of Cr(II) NHC complexes.^{66–77} The *trans* C1–Cr–C1' and C2–Cr–C2' angles are 170.54(14)° and 177.39(12)°, respectively, and the Cr atom sits on the calculated centroid of the plane of the NHC carbenes.

The significant electronic unsaturation of complex **2** combined with its low valent state makes **2** an excellent choice for oxidative group transfer reactions. The oxidation of **2** with nitrogen or oxygen transfer reagents should yield Cr(IV) complexes with metal–ligand multiple bonds, which are quite rare.^{33–44} The reactions of **2** with Me_3NO and molecular O_2

gave $[(\text{BMe}_2\text{EtTC}^H)\text{Cr}(\text{O})]$ (**3**), as pale green crystals in 14% and 50% yield, respectively (Scheme 1), showcasing the chromium(II) complex's ability to activate O_2 . Complex **3** is paramagnetic on the basis of ^1H NMR. Previously isolated terminal Cr(IV) oxos have exhibited both diamagnetism (a porphyrin complex by Groves⁴² and a cyclam complex by Nam⁴¹) and paramagnetism (two siloxide chromium complexes by Wolczanski³⁸ and two Tp complexes by Theopold^{43,44}). Complex **3** has a strong stretch in the IR spectrum at 1031 cm^{-1} which can be attributed to the terminal oxo, and is consistent with porphyrin and corrole based Cr oxo complexes.^{22–24,40,42,78} Single crystal X-ray data reveals a square pyramidal geometry for **3** with the Cr atom raised 0.525 Å above the plane of the carbene carbons (Figure 3). The Cr–C

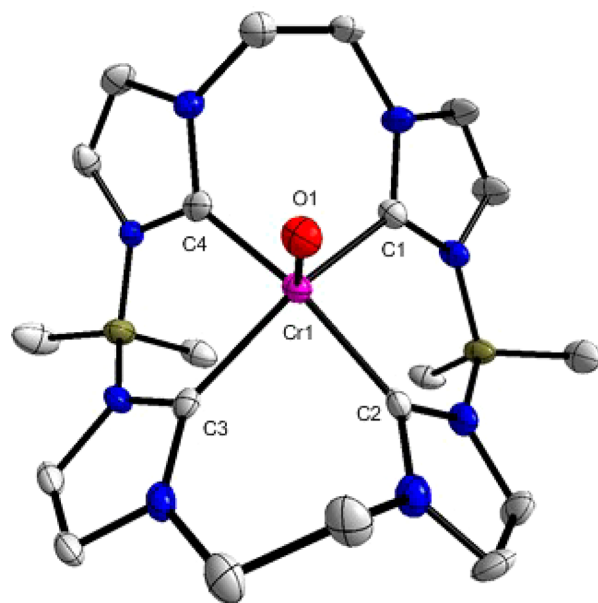
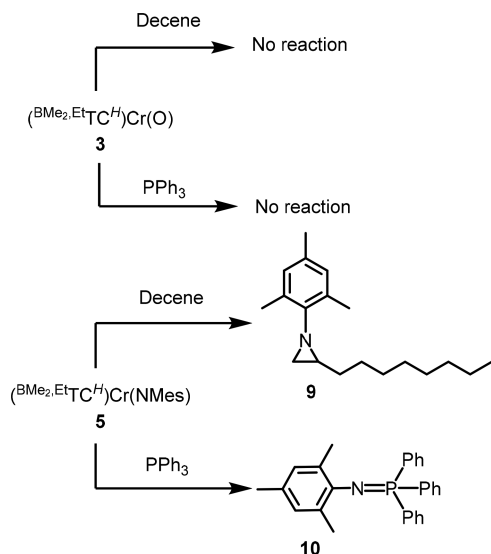


Figure 3. X-ray crystal structure of $[(\text{BMe}_2\text{EtTC}^H)\text{Cr}(\text{O})]$, **3**. Purple, red, blue, gray, and olive ellipsoids (30% probability) represent Cr, O, N, C, and B atoms, respectively. Solvent molecules and H atoms are omitted for clarity. Selected interatomic bond distances (Å) and angles (deg) are as follows: Cr1–C1 = 2.094(5); Cr1–C2 = 2.031(5); Cr1–C3 = 2.080(5); Cr1–C4 = 2.026(5); Cr1–O1 = 1.564(3); C4–Cr1–C2 = 153.3(2); C3–Cr1–C1 = 147.7(2).

bond distances range from 2.026 to 2.094 Å which is significantly shorter than the distances observed for **2**, while the *trans* C–Cr–C bond angles show only a mild distortion from a bent square pyramidal geometry.

Since the few examples of terminal Cr(IV) oxos have shown a wide range of reactivity, from highly stable to radical reactions with C–H bonds, we tested **3** to elucidate its group transfer potential.^{17,39,44} A test reaction with **3** and 1-decene showed no reactivity toward epoxidation (Scheme 2). In a similar manner, test reactions with **3** and triphenylphosphine showed no reaction. These results are consistent with Che's Cr(IV) oxo supported by a porphyrin auxiliary ligand in a square pyramidal geometry.⁷⁹ In contrast, Theopold has shown that a tris-(pyrazolyl)borate based Cr(IV) oxo complex in trigonal bipyramidal geometry is capable of hydrogen atom abstraction through activation of weak C–H bonds.⁴⁴ The Cr–O distance of 1.564 Å is the shortest bond for a chromium(IV) oxo and combined with its no further reactivity toward group transfer indicates a triple bond character between Cr and O.^{40–44}

Scheme 2. Group Transfer Reactions with 3 (Top) and 5 (Bottom)



In addition to chromium oxos, we were particularly interested in the formation of multivalent chromium imidos. Metal imidos are purported intermediates during catalytic aziridination, and an isostructural iron complex to 2 was recently reported to be the first general catalyst for the formation of aziridines from alkyl azides.⁸ A variety of organic azides were tested for potential conversion to imidos, which yielded a diversity of structural motifs.

The reaction of 2 with tolyl azide yielded not the expected chromium imido, but a metallotetrazene, 4 (Scheme 1). The metallotetrazene is presumably formed in a [2 + 3] cycloaddition by addition of an additional equivalent of organic azide with a transient metal imido.¹⁰ The Cr–C bond distances range from 2.056 to 2.120 Å which is in the expected range (Figure 4). Tetrazenes are noninnocent ligands which potentially make the oxidation state assignment of the Cr metal center ambiguous.^{80–82} A comparison of the N–N bond distances in the tetrazene shows that the N2–N3 bond distance (1.287 Å) is shorter than the N1–N2 (1.364 Å) and N3–N4 (1.359 Å) distances which suggests that there is a double bond between the central nitrogens. This would make the tetrazene

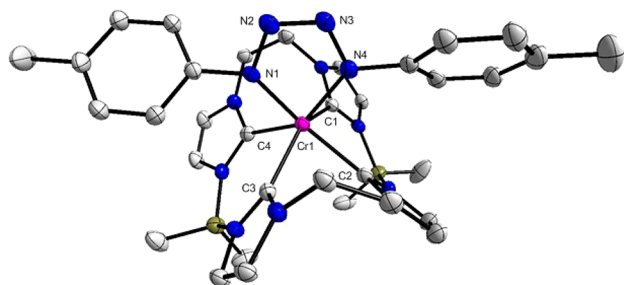


Figure 4. X-ray crystal structure of $[(\text{BMe}_2\text{EtTC}^H)\text{Cr}((p\text{-tolyl})\text{N}_4(p\text{-tolyl}))]$, 4. Purple, blue, gray, and olive ellipsoids (50% probability) represent Cr, N, C, and B atoms, respectively. Selected interatomic bond distances (Å) and angles (deg) are as follows: Cr1–C1 = 2.056(3); Cr1–C2 = 2.120(3); Cr1–C3 = 2.063(3); Cr1–C4 = 2.118(3); Cr1–N1 = 1.977(3); Cr1–N4 = 1.964(3); N1–N2 = 1.359(3); N2–N3 = 1.287(3); N3–N4 = 1.358(3); C4–Cr1–C2 = 121.82(11); C1–Cr1–C3 = 140.41(11).

ligand in 4 dianionic and not radical in nature which is consistent with our previous studies on isostructural iron tetrazenes.¹⁰ Previously reported Cr(III) tetrazenes have similar double bond character on the central nitrogens.^{80,81} As a consequence of attempting to relieve steric hindrance, the crystal structure of 4 is slightly distorted from a trigonal prismatic geometry ($\phi_{\text{av}} = 7.77^\circ$, perfect trigonal prism, $\phi = 0^\circ$). This distortion can also be observed in the distinction between the two trans C–Cr–C angles which are quite disparate (C4–Cr–C2 = 121.8(1)° and C1–Cr–C3 = 140.4(1)°).

Since sterically bulky azides can hinder the formation of a metallotetrazene, we reacted 1 equiv of mesityl azide with 2 which resulted in an isolable Cr-imido complex 5 in 50% yield (Scheme 1). The red-orange compound 5 is a paramagnetic species as revealed by its ¹H NMR, which showed all eight expected peaks. While many chromium imidos have been previously prepared, only eight examples of Cr(IV) imidos are known.^{34–39,83,84} These Cr(IV) imido complexes are all diamagnetic, except the three trigonal examples reported by Groyzman, the pseudotrigonal example by Wolczanski and co-workers, and the only square pyramidal complex made by West.⁸⁴

The X-ray structure reveals that 5 adopts a bent square pyramidal geometry with the central Cr atom sitting 0.542 Å out of the tetracarbene plane (Figure 5). The Cr–C bond

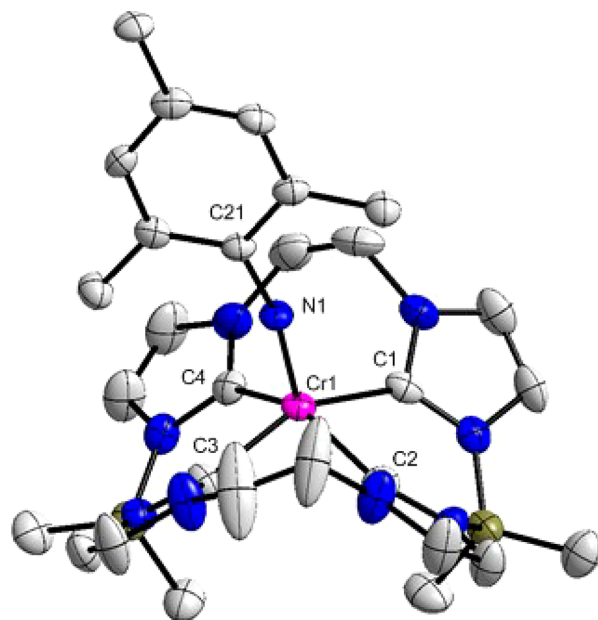


Figure 5. X-ray crystal structure of $[(\text{BMe}_2\text{EtTC}^H)\text{Cr}(\text{NMes})]$, 5. Purple, blue, gray, and olive ellipsoids (50% probability) represent Cr, N, C, and B atoms, respectively. Selected interatomic bond distances (Å) and angles (deg) are as follows: Cr1–C1 = 2.104(6); Cr1–C2 = 2.097(6); Cr1–C3 = 2.065(6); Cr1–C4 = 2.082(6); Cr1–N1 = 1.703(4); N1–C21 = 1.386(6); C4–Cr1–C2 = 147.81(2); C3–Cr1–C1 = 151.8(2); C21–N1–Cr1 = 166.1(4).

distances range from 2.067 to 2.102 Å which is between the values for 3 and 4. The Cr–N1 bond distance of 1.704 Å in 5 is the longest Cr(IV)-imido bond to date. In addition, the N1–C21 distance is also extended to 1.386 Å which is longer than a typical single bond. These bond distances combined with the slightly bent Cr1–N1–C21 angle of 166.2° indicate a delocalized double bond, which is in contrast to the eight

other examples of Cr(IV) imidos.^{34–36,38,39,83,84} The closest example of a similar imido complex is a Ta species reported by Bercaw in 1992 that showcased a double bond character with a nearly linear geometry on the metal-imido bond due to the lone pair on nitrogen residing on the empty p orbital instead of an sp or an sp² hybridized orbital.³⁷ This distinct structural difference between **3** and **5** suggested to us that **5** would be more effective for group transfer since it does not have a metal–ligand triple bond like **3**.

While there are almost no examples of successful group transfer reactions from Cr(IV) imido complexes,³⁹ several high valent chromium imidos showed reactivity toward hydrogen abstraction and imido group transfer to phosphines.²⁰ We tested complex **5** for nitrene group transfer with 1-decene and PPh₃ to form the corresponding aziridine and triphenylphosphanimine, respectively. Stoichiometric addition of 1-decene to **5** at 75 °C in benzene yielded 1-(mesityl)-2-octylaziridine, **9**, in 86% yield (Scheme 2). This formation of aziridine from an imido and an alkene is the first successful group transfer of this type with chromium. In a similar manner, addition of triphenylphosphine to **5** yields *N*-mesityl-1,1,1-triphenylphosphanimine, **10**, in 65% yield. Since both the oxidative group transfer and reductive elimination of the imido are successful, **2** appeared to be a potential catalyst for aziridination, at least with sterically bulky azides. Nonetheless, the catalytic reaction with mesityl azide, decene, and **2** was not successful. Further investigations revealed this was because **2** was susceptible to thermal degradation at 75 °C.

Since alkyl azides are more challenging to activate compared to aryl azides,^{85–87} we tested the effectiveness of oxidative group transfer of these reagents with **2**. The reaction of *n*-octyl azide with **2** resulted in a metallotetrazene, [(^{BMe₃,Et}Tc^H)Cr((*n*-octyl)₄(*n*-octyl))], **6**, that is analogous to **4** (Scheme 1). The crystal structure showed that **6** has trigonal prismatic geometry with a modest distortion ($\phi_{av} = 8.62^\circ$), similar to **4** (Figure 6). The distortion for complex **6** is slightly higher than that of **4** due to increased steric repulsion imposed by bulkier alkyl

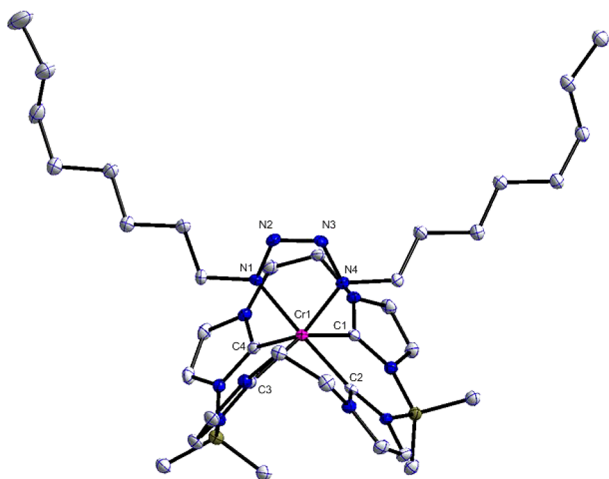


Figure 6. X-ray crystal structure of [(^{BMe₃,Et}Tc^H)Cr((*n*-octyl)₄(*n*-octyl))], **6**. Purple, blue, gray, and olive ellipsoids (50% probability) represent Cr, N, C, and B atoms, respectively. Selected interatomic bond distances (Å) and angles (deg) are as follows: Cr1–C1 = 2.0701(19); Cr1–C2 = 2.1288(19); Cr1–C3 = 2.0879(19); Cr1–C4 = 2.1591(19); Cr1–N1 = 1.9644(16); N1–N2 = 1.347(2); N2–N3 = 1.303(2); N3–N4 = 1.347(2); Cr1–N4 = 1.9531(16); C1–Cr1–C3 = 141.79 (7); C2–Cr1–C4 = 126.68(7).

substituents. A comparison of the N–N bond distances on the tetrazene ligand shows that the central nitrogen bond distance for N2–N3 (1.303 Å) is shorter compared to the other two nitrogen bond distances, N1–N2 (1.347 Å) and N3–N4 (1.347 Å).

Shifting to a bulkier alkyl azide formed the expected chromium imido complex. The reaction of adamantyl azide and **2** gave [(^{BMe₃,Et}Tc^H)Cr(NAd)], **7** (Figure 7), albeit in only

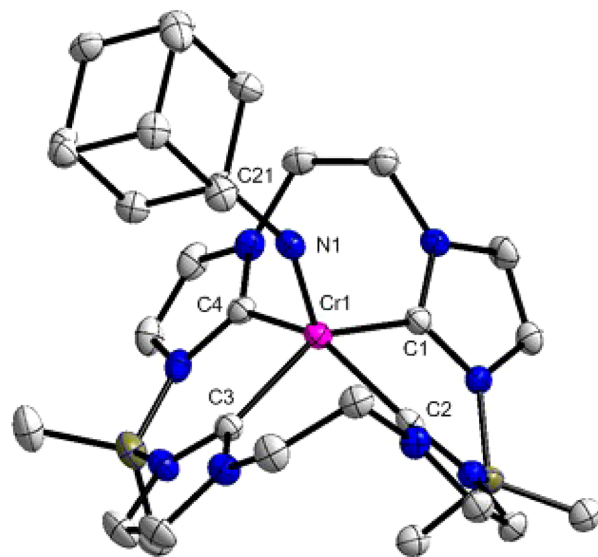


Figure 7. X-ray crystal structure of [(^{BMe₃,Et}Tc^H)Cr(NAd)], **7**. Purple, blue, gray, and olive ellipsoids (50% probability) represent Cr, N, C, and B atoms, respectively. Selected interatomic bond distances (Å) and angles (deg) are as follows: Cr1–C1 = 2.096(3); Cr1–C2 = 2.101(3); Cr1–C3 = 2.070(3); Cr1–C4 = 2.066(3); Cr1–N1 = 1.686(2); N1–C21 = 1.453(4); C4–Cr1–C2 = 143.9(11); C3–Cr1–C1 = 142.0(11); Cr1–N1–C21 = 149.8(2).

20% yield (Scheme 1). A comparison of the crystal structures of **5** and **7** shows that they are similar except for the bonding of the imido ligand. The Cr–N1 bond distance on **7** is 1.686 Å which is slightly shorter than the Cr–N1 distance on **5**, but the bond angle for Cr1–N1–C21 of 149.8° is considerably more bent. Complex **7** has one of the most bent Cr–N–C angles for a Cr(IV) imido complex while all of the other examples are nearly linear.^{34–36,38,39,83} The combination of an elongated Cr–N1 bond and a bent Cr1–N1–C21 angle is consistent with a chromium imido double bond.

In addition to the reactions with organic azides, we tested a reaction of **2** with TMS-azide. The TMS group is an easily removable protecting group, and it has been employed as a surrogate for hydrazoic acid.⁸⁸ However, instead of isolating the expected imido or tetrazene complex, a reaction of **2** and excess TMS-azide yielded a bis-chromium bridging nitrido complex, [(^{BMe₃,Et}Tc^H)Cr]₂(N), **8**, in 50% yield (Scheme 1). While TMS-azide has not been demonstrated to form bridging nitridos previously, there are examples where TMS-azide forms terminal nitridos.⁸⁹ Sodium azide has been demonstrated to form bridging nitridos by delivering an azide to the metal which is followed by attack of a second transition metal with the extrusion of N₂.^{90,91} A similar reaction pathway could explain the synthesis of **8**, where TMS-azide acts as a radical azide transfer agent to the first equivalent of **2**, followed by attack of a second equivalent of **2** and loss of N₂. These combined oxidation processes would lead to Cr1 and Cr2 metal centers at

+4 and +3 oxidation states, respectively. The X-ray structural data for **8** revealed an asymmetric bridging nitrido ligand (Cr1–N1 = 1.667 Å versus Cr2–N1 = 1.899 Å) (Figure 8).

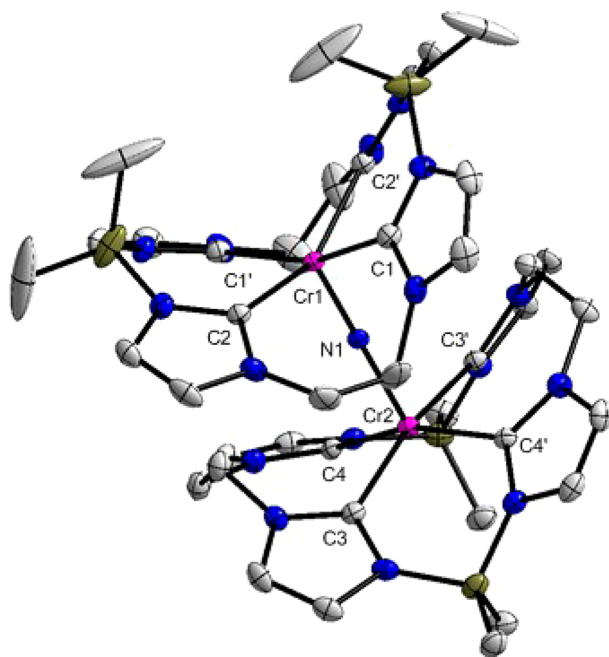


Figure 8. X-ray crystal structure of $[(^{BMe_2Et}TC^H)Cr]_2(N)$, **8**. Purple, blue, gray, and olive ellipsoids (30% probability) represent Cr, N, C, and B atoms, respectively. Selected interatomic bond distances (Å) and angles (deg) are as follows: Cr1–C1 = 2.086(5); Cr1–C2 = 2.111(4); Cr2–C3 = 2.104(4); Cr2–C4 = 2.163(4); Cr1–N1 = 1.667(5); Cr2–N1 = 1.896(5); C1–Cr1–C1' = 158.80 (2); C2–Cr1–C2' = 153.4(2); C3–Cr2–C3' = 168.4(2); C4–Cr2–C4' = 160.5(2); Cr1–N1–Cr2 = 180.

The Cr1–N1–Cr2 angle is a perfect 180° showing a linear arrangement between the bridging nitrido and the two metal centers. The Cr1–C bond distances are shorter (Cr1–C1 = 2.082 Å, Cr1–C2 = 2.120 Å) compared to the Cr2–C bond distances (Cr2–C3 = 2.104 Å, Cr2–C4 = 2.167 Å) which supports the assertion that the metals are in different oxidation states. To our knowledge, complex **8** is the first isolable, bridging linear nitrido monomeric chromium complex. A dimeric chromium(V) complex⁹⁸ with bridging nitrido forming a diamond core has been reported by Cummins and coworkers while Wieghardt and co-workers in a previous report mention a possible Cr(III)/Cr(V) mixed valent bridging nitrido species, solely based on spectroscopic evidence, which was formed from a photo-decomposition reaction.⁹² This proposed species was never isolated. Complex **8** is particularly noteworthy since there are numerous examples of linear bridging nitridos on vanadium and iron on the first row, and molybdenum and tungsten in the same column.^{91–97}

Since **8** is the first isolated bridging mononitrido on chromium and bridging nitridos and oxos are so critical in magnetic materials, we decided to test the magnetic interactions between the chromium centers. Variable temperature dc susceptibility measurements for **8** were collected (5–300 K) at 1 T (Figure 9). The resulting susceptibility curve achieves a maximum value just below 1.7 cm³ K mol⁻¹ at low temperature before declining toward the spin-only value for two, non-interacting spin centers with $S = 1$ and $S = 0.5$ (1.375 cm³ K

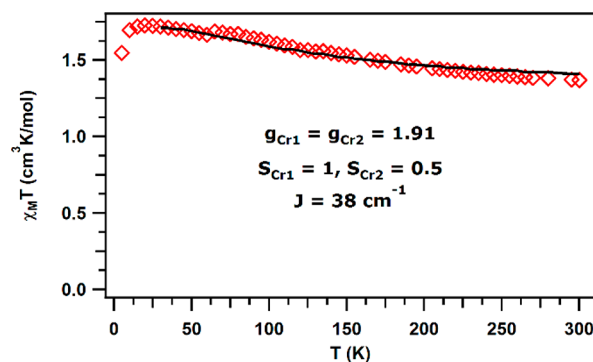


Figure 9. Variable temperature dc magnetic susceptibility for **8**. $\chi_M T$ vs T plot shown. Data was collected at 1.0 T. Fit parameters obtained with PHI: $g_{Cr1} = g_{Cr2} = 1.91$, $J = 38 \text{ cm}^{-1}$.

mol⁻¹). An alternative interpretation could be a set of $S = 3/2$ and $S = 0$ metal centers, but that should have a value of 1.87 cm³ K mol⁻¹ and should yield a flat line for the magnetic susceptibility independent of temperature. The increasing magnetic susceptibility as temperature was lowered is suggestive of a Cr(III)/Cr(IV) pair with weak ferromagnetic coupling. A fit of the data with PHI⁶² according to this model produced a satisfactory fit and yielded a coupling constant, J , of 38 cm⁻¹.

CONCLUSIONS

In conclusion, we have isolated and structurally characterized a diverse family of chromium(IV) complexes that demonstrates the distinctions in reactivity between different oxidative group transfer reagents. The initial low valent square planar tetracarbenes complex, **2**, was synthesized by an in situ deprotonation strategy using ⁿBuLi on a macrocyclic tetraimidazolium and CrCl₂. This highly electronically unsaturated complex provides an extremely versatile synthon to generate various multiply bonded metal–ligand chromium complexes including a Cr(IV)-oxo, **3**, Cr(IV)-imidos, **5** and **7**, and the first bridging mononitrido Cr(III)/Cr(IV), **8**. In addition to the chromium–ligand multiple bond species, less sterically bulky organic azides lead to Cr(IV) metallotetrazenes, **4** and **7**. A comparison of the bond distances obtained by X-ray diffraction demonstrates that the oxo complex has a stronger π donation compared to the imido ligands, resulting in a triple bond for **3** versus double bonds for **5** and **7**. This conclusion on the difference in bond order is corroborated with reactivity studies. The oxo complex, **3**, shows no group transfer reactivity, while the mesityl imido complex, **5**, yields an aziridine in the presence of 1-decene. This aziridination is the first reported formation of an aziridine directly from a chromium imido complex. Although numerous oxo and imido complexes of chromium have been reported previously, the vast majority of them were high valent (Cr(V) and Cr(VI)) and showed little to no reactivity toward reductive group transfer. Finally, we investigated the first linearly bridging nitrido of a bis-chromium complex. This complex, **8**, has two inequivalent chromium centers based on X-ray crystallography and SQUID magnetometry and exhibits weak ferromagnetic coupling. This study is an unprecedented comparison of oxidative group transfer reactions on low valent chromium that is supported by a single auxiliary ligand platform. Insights from this research can lead to improved development of catalytic redox reactions on midvalent chromium.

■ ASSOCIATED CONTENT

● Supporting Information

The Supporting Information is available free of charge on the ACS Publications website at DOI: 10.1021/acs.inorgchem.7b02253.

High resolution mass spectra and X-ray crystallographic data tables (PDF)

■ Accession Codes

CCDC 1582056–1582062 contain the supplementary crystallographic data for this paper. These data can be obtained free of charge via www.ccdc.cam.ac.uk/data_request/cif, or by emailing data_request@ccdc.cam.ac.uk, or by contacting The Cambridge Crystallographic Data Centre, 12 Union Road, Cambridge CB2 1EZ, UK; fax: +44 1223 336033.

■ AUTHOR INFORMATION

■ Corresponding Author

*E-mail: jenkins@ion.chem.utk.edu.

■ ORCID

David M. Jenkins: 0000-0003-2683-9157

■ Notes

The authors declare no competing financial interest.

■ ACKNOWLEDGMENTS

The authors gratefully acknowledge the National Science Foundation (NSF-CAREER/CHE-1254536) for financial support of this work.

■ REFERENCES

- (1) Yoshizawa, K. Nonradical mechanism for methane hydroxylation by iron-oxo complexes. *Acc. Chem. Res.* **2006**, *39*, 375–382.
- (2) Ye, S. F.; Neese, F. Nonheme oxo-iron(IV) intermediates form an oxyl radical upon approaching the C-H bond activation transition state. *Proc. Natl. Acad. Sci. U. S. A.* **2011**, *108*, 1228–1233.
- (3) Chen, K.; Que, L., Jr. Evidence for the participation of a high-valent iron-oxo species in stereospecific alkane hydroxylation by a nonheme iron catalyst. *Chem. Commun.* **1999**, 1375–1376.
- (4) Geng, C. Y.; Ye, S. F.; Neese, F. Analysis of Reaction Channels for Alkane Hydroxylation by Nonheme Iron(IV)-Oxo Complexes. *Angew. Chem., Int. Ed.* **2010**, *49*, 5717–5720.
- (5) Tang, H.; Guan, J.; Zhang, L. L.; Liu, H. L.; Huang, X. R. The effect of the axial ligand on distinct reaction tunneling for methane hydroxylation by nonheme iron(IV)-oxo complexes. *Phys. Chem. Chem. Phys.* **2012**, *14*, 12863–12874.
- (6) Nam, W.; Goh, Y. M.; Lee, Y. J.; Lim, M. H.; Kim, C. Biomimetic alkane hydroxylations by an iron(III) porphyrin complex with H₂O₂ and by a high-valent iron(IV) oxo porphyrin cation radical complex. *Inorg. Chem.* **1999**, *38*, 3238–3240.
- (7) Ballou, D. P.; Coulter, E. D.; Isaac, I. S.; Beharry, Z. M.; Dawson, J. H. Spectroscopic evidence for the formation of an oxo-iron(IV) complex during the peracid-dependent hydroxylation of 5,5-difluorocamphor by cytochrome P450-CAM. *Faseb. J.* **1997**, *11*, A783–A783.
- (8) Chandrachud, P. P.; Bass, H. M.; Jenkins, D. M. Synthesis of Fully Aliphatic Aziridines with a Macrocyclic Tetracarbene Iron Catalyst. *Organometallics* **2016**, *35*, 1652–1657.
- (9) Cramer, S. A.; Jenkins, D. M. Synthesis of Aziridines from Alkenes and Aryl Azides with a Reusable Macrocyclic Tetracarbene Iron Catalyst. *J. Am. Chem. Soc.* **2011**, *133*, 19342–19345.
- (10) Cramer, S. A.; Sanchez, R. H.; Brakhage, D. F.; Jenkins, D. M. Probing the role of an Fe-IV tetrazene in catalytic aziridination. *Chem. Commun.* **2014**, *50*, 13967–13970.
- (11) Jenkins, D. M. Atom-Economical C-2+N-1 Aziridination: Progress towards Catalytic Intermolecular Reactions Using Alkenes and Aryl Azides. *Synlett* **2012**, *23*, 1267–1270.
- (12) King, E. R.; Hennessy, E. T.; Betley, T. A. Catalytic C-H Bond Amination from High-Spin Iron Imido Complexes. *J. Am. Chem. Soc.* **2011**, *133*, 4917–4923.
- (13) Mahy, J. P.; Battioni, P.; Mansuy, D. Formation of an Iron(III) Porphyrin Complex with a Nitrene Moiety Inserted into a Fe-N Bond during Alkene Aziridination by [(Tosylimido)Iodo]Benzene Catalyzed by Iron(III) Porphyrins. *J. Am. Chem. Soc.* **1986**, *108*, 1079–1080.
- (14) Jensen, M. P.; Lange, S. J.; Mehn, M. P.; Que, E. L.; Que, L. Biomimetic aryl hydroxylation derived from alkyl hydroperoxide at a nonheme iron center. Evidence for an Fe-IV=O oxidant. *J. Am. Chem. Soc.* **2003**, *125*, 2113–2128.
- (15) Nam, W. Synthetic Mononuclear Nonheme Iron-Oxygen Intermediates. *Acc. Chem. Res.* **2015**, *48*, 2415–2423.
- (16) Che, C. M.; Lo, V. K. Y.; Zhou, C. Y.; Huang, J. S. Selective functionalisation of saturated C-H bonds with metalloporphyrin catalysts. *Chem. Soc. Rev.* **2011**, *40*, 1950–1975.
- (17) Cho, K. B.; Kang, H.; Woo, J.; Park, Y. J.; Seo, M. S.; Cho, J.; Nam, W. Mechanistic Insights into the C-H Bond Activation of Hydrocarbons by Chromium(IV) Oxo and Chromium(III) Superoxo Complexes. *Inorg. Chem.* **2014**, *53*, 645–652.
- (18) Kotani, H.; Kaida, S.; Ishizuka, T.; Sakaguchi, M.; Ogura, T.; Shiota, Y.; Yoshizawa, K.; Kojima, T. Formation and characterization of a reactive chromium(V)-oxo complex: mechanistic insight into hydrogen-atom transfer reactions. *Chem. Sci.* **2015**, *6*, 945–955.
- (19) Liu, S.; Mase, K.; Bougher, C.; Hicks, S. D.; Abu-Omar, M. M.; Fukuzumi, S. High-Valent Chromium-Oxo Complex Acting as an Efficient Catalyst Precursor for Selective Two-Electron Reduction of Dioxxygen by a Ferrocene Derivative. *Inorg. Chem.* **2014**, *53*, 7780–7788.
- (20) Zhou, W.; Patrick, B. O.; Smith, K. M. Influence of redox non-innocent phenylenediamido ligands on chromium imido hydrogen-atom abstraction reactivity. *Chem. Commun.* **2014**, *50*, 9958–9960.
- (21) Cho, J.; Woo, J.; Han, J. E.; Kubo, M.; Ogura, T.; Nam, W. Chromium(V)-oxo and chromium(III)-superoxo complexes bearing a macrocyclic TMC ligand in hydrogen atom abstraction reactions. *Chem. Sci.* **2011**, *2*, 2057–2062.
- (22) Edwards, N. Y.; Eikey, R. A.; Loring, M. I.; Abu-Omar, M. M. High-Valent Imido Complexes of Manganese and Chromium Corroles. *Inorg. Chem.* **2005**, *44*, 3700–3708.
- (23) Egorova, O. A.; Tsay, O. G.; Khatua, S.; Huh, J. O.; Churchill, D. G. A Chiral meso-ABC-Corrolatochromium(V) Complex. *Inorg. Chem.* **2009**, *48*, 4634–4636.
- (24) Meier-Callahan, A. E.; Gray, H. B.; Gross, Z. Stabilization of High-Valent Metals by Corroles: Oxo[tris(pentafluorophenyl)-corrolato]chromium(V). *Inorg. Chem.* **2000**, *39*, 3605–3607.
- (25) Noh, S. K.; Heintz, R. A.; Haggerty, B. S.; Rheingold, A. L.; Theopold, K. H. Oxo-alkyls of chromium(V) and chromium(VI). *J. Am. Chem. Soc.* **1992**, *114*, 1892–1893.
- (26) Siddall, T. L.; Miyaura, N.; Huffman, J. C.; Kochi, J. K. Isolation and molecular structure of unusual oxochromium(V) cations for the catalytic epoxidation of alkenes. *J. Chem. Soc., Chem. Commun.* **1983**, 1185–1186.
- (27) Srinivasan, K.; Kochi, J. K. Synthesis and molecular structure of oxochromium(V) cations: Coordination with donor ligands. *Inorg. Chem.* **1985**, *24*, 4671–4679.
- (28) Wistuba, T.; Limberg, C.; Kircher, P. Trapping of an Organic Radical by an O=Cr^{VI} Function. *Angew. Chem., Int. Ed.* **1999**, *38*, 3037–3039.
- (29) Hess, J. S.; Leelasubcharoen, S.; Rheingold, A. L.; Doren, D. J.; Theopold, K. H. Spin Surface Crossing in Chromium-Mediated Olefin Epoxidation with O₂. *J. Am. Chem. Soc.* **2002**, *124*, 2454–2455.
- (30) Monillas, W. H.; Yap, G. P. A.; MacAdams, L. A.; Theopold, K. H. Binding and Activation of Small Molecules by Three-Coordinate Cr(I). *J. Am. Chem. Soc.* **2007**, *129*, 8090–8091.
- (31) Subramaniam, P.; Anbarasan, S.; Devi, S. S.; Ramdass, A. Modulation of catalytic activity by ligand oxides in the sulfoxidation of phenylmercaptoacetic acids by oxo(salen)chromium(V) complexes. *Polyhedron* **2016**, *119*, 14–22.

- (32) Theopold, K. H. In *Organometallic Oxidation Catalysis*; Meyer, F., Limberg, C., Eds.; Springer-Verlag: Berlin, 2007; Vol. 22, pp 17–37.
- (33) Barron, A. R.; Salt, J. E.; Wilkinson, G.; Motevalli, M.; Hursthouse, M. B. The chemistry of chromium nitrile complexes of 1,2-bis(dimethylphosphino)-ethane. X-Ray crystal structures of trans-[CrCl(NEt)(dmpe)₂]CF₃SO₃, trans-[Cr(N=CHMe)₂(dmpe)₂]-[BPh₄]₂, and trans-[Co⁰(HNCMe)₂(dmpe)₂][BPh₄]₂. *J. Chem. Soc., Dalton Trans.* **1987**, 2947–2954.
- (34) Beaumier, E. P.; Billow, B. S.; Singh, A. K.; Biros, S. M.; Odom, A. L. A complex with nitrogen single, double, and triple bonds to the same chromium atom: synthesis, structure, and reactivity. *Chem. Sci.* **2016**, 7, 2532–2536.
- (35) Danopoulos, A. A.; Wilkinson, G.; Sweet, T. K. N.; Hursthouse, M. B. Reactions of bis(mesitylimido)bis(arylthiolato)chromium(VI) compounds. *Polyhedron* **1996**, 15, 873–879.
- (36) Lu, C. C.; DeBeer George, S.; Weyhermüller, T.; Bill, E.; Bothe, E.; Wieghardt, K. An Electron-Transfer Series of High-Valent Chromium Complexes with Redox Non-Innocent, Non-Heme Ligands. *Angew. Chem., Int. Ed.* **2008**, 47, 6384–6387.
- (37) Parkin, G.; Van Asselt, A.; Leahy, D. J.; Whinnery, L.; Hua, N. G.; Quan, R. W.; Henling, L. M.; Schaefer, W. P.; Santarsiero, B. D.; Bercaw, J. E. Oxo-hydrido and imido-hydrido derivatives of permethyltantaloene. Structures of (η^5 -C₅Me₅)₂Ta(=O)H and (η^5 -C₅Me₅)₂Ta(=NC₆H₅)H: Doubly or triply bonded tantalum oxo and imido ligands? *Inorg. Chem.* **1992**, 31, 82–85.
- (38) Sydora, O. L.; Kuiper, D. S.; Wolczanski, P. T.; Lobkovsky, E. B.; Dinescu, A.; Cundari, T. R. The Butterfly Dimer [(^tBu₃SiO)-Cr]₂(μ -OSi^tBu₃)₂ and Its Oxidative Cleavage to (^tBu₃SiO)₂Cr(N-NCPh₂)₂ and (^tBu₃SiO)₂CrN(2,6-Ph₂-C₆H₃). *Inorg. Chem.* **2006**, 45, 2008–2021.
- (39) Yousif, M.; Tjapkes, D. J.; Lord, R. L.; Groysman, S. Catalytic Formation of Asymmetric Carbodiimides at Mononuclear Chromium-(II/IV) Bis(alkoxide) Complexes. *Organometallics* **2015**, 34, 5119–5128.
- (40) Budge, J. R.; Gatehouse, B. M. K.; Nesbit, M. C.; West, B. O. The autoxidation of a chromium (II) porphyrin: synthesis and structural characterisation by X-ray crystallography of $\alpha\beta\gamma\delta$ -tetraphenyl-porphinato-oxochromium(IV). *J. Chem. Soc., Chem. Commun.* **1981**, 370–371.
- (41) Cho, J.; Woo, J.; Nam, W. A Chromium(III)–Superoxo Complex in Oxygen Atom Transfer Reactions as a Chemical Model of Cysteine Dioxygenase. *J. Am. Chem. Soc.* **2012**, 134, 11112–11115.
- (42) Groves, J. T.; Kruper, W. J.; Haushalter, R. C.; Butler, W. M. Synthesis, characterization, and molecular structure of oxo-(porphyrinato)chromium(IV) complexes. *Inorg. Chem.* **1982**, 21, 1363–1368.
- (43) Hess, A.; Horz, M. R.; Liable-Sands, L. M.; Lindner, D. C.; Rheingold, A. L.; Theopold, K. H. Insertion of O₂ into a chromium-phenyl bond: Mechanism of formation of the paramagnetic d² oxo complex Tp(^tBu₂Me)Cr(IV)(O)OPh. *Angew. Chem., Int. Ed.* **1999**, 38, 166–168.
- (44) Qin, K.; Incarvito, C. D.; Rheingold, A. L.; Theopold, K. H. Hydrogen atom abstraction by a chromium(IV) oxo complex derived from O₂. *J. Am. Chem. Soc.* **2002**, 124, 14008–14009.
- (45) Hickey, A. K.; Lutz, S. A.; Chen, C. H.; Smith, J. M. Two-state reactivity in C-H activation by a four-coordinate iron(0) complex. *Chem. Commun.* **2017**, 53, 1245–1248.
- (46) Lin, H. J.; Siretanu, D.; Dickie, D. A.; Subedi, D.; Scepianiak, J. J.; Mitcov, D.; Clerac, R.; Smith, J. M. Steric and Electronic Control of the Spin State in Three-Fold Symmetric, Four-Coordinate Iron(II) Complexes. *J. Am. Chem. Soc.* **2014**, 136, 13326–13332.
- (47) Mankad, N. P.; Muller, P.; Peters, J. C. Catalytic N-N Coupling of Aryl Azides To Yield Azoarenes via Trigonal Bipyramid Iron-Nitrene Intermediates. *J. Am. Chem. Soc.* **2010**, 132, 4083–4085.
- (48) Mehn, M. P.; Peters, J. C. Mid- to high-valent imido and nitrido complexes of iron. *J. Inorg. Biochem.* **2006**, 100, 634–643.
- (49) Nieto, I.; Ding, F.; Bontchev, R. P.; Wang, H. B.; Smith, J. M. Thermodynamics of hydrogen atom transfer to a high-valent iron imido complex. *J. Am. Chem. Soc.* **2008**, 130, 2716.
- (50) Saouma, C. T.; Peters, J. C. M E and M = E complexes of iron and cobalt that emphasize three-fold symmetry (E O, N, NR). *Coord. Chem. Rev.* **2011**, 255, 920–937.
- (51) Smith, J. M.; Subedi, D. The structure and reactivity of iron nitride complexes. *Dalton Trans.* **2012**, 41, 1423–1429.
- (52) Meyer, S.; Krahe, O.; Kupper, C.; Klawitter, I.; Demeshko, S.; Bill, E.; Neese, F.; Meyer, F. A trans-1,2 End-On Disulfide-Bridged Iron-Tetracarbene Dimer and Its Electronic Structure. *Inorg. Chem.* **2015**, 54, 9770–9776.
- (53) Meyer, S.; Orben, C. M.; Demeshko, S.; Dechert, S.; Meyer, F. Synthesis and Characterization of Di- and Tetracarbene Iron(II) Complexes with Chelating N-Heterocyclic Carbene Ligands and Their Application in Aryl Grignard-Alkyl Halide Cross-Coupling. *Organometallics* **2011**, 30, 6692–6702.
- (54) Ye, S. F.; Kupper, C.; Meyer, S.; Andris, E.; Navratil, R.; Krahe, O.; Mondal, B.; Atanasov, M.; Bill, E.; Roithova, J.; Meyer, F.; Neese, F. Magnetic Circular Dichroism Evidence for an Unusual Electronic Structure of a Tetracarbene-Oxoiron(IV) Complex. *J. Am. Chem. Soc.* **2016**, 138, 14312–14325.
- (55) Lu, Z.; Cramer, S. A.; Jenkins, D. M. Exploiting a dimeric silver transmetallating reagent to synthesize macrocyclic tetracarbene complexes. *Chem. Sci.* **2012**, 3, 3081–3087.
- (56) Bass, H. M.; Cramer, S. A.; McCullough, A. S.; Bernstein, K. J.; Murdock, C. R.; Jenkins, D. M. Employing Dianionic Macrocyclic Tetracarbenes To Synthesize Neutral Divalent Metal Complexes. *Organometallics* **2013**, 32, 2160–2167.
- (57) Bruker APEX2; Bruker AXS Inc.: Madison, WI, 2012.
- (58) Sheldrick, G. M. SADABS; University of Göttingen: Göttingen, Germany, 1996.
- (59) Sheldrick, G. M. *Acta Crystallogr., Sect. A: Found. Adv.* **2015**, A71, 3–8.
- (60) Dolomanov, O. V.; Bourhis, L. J.; Gildea, R. J.; Howard, J. A. K.; Puschmann, H. OLEX2: a complete structure solution, refinement and analysis program. *J. Appl. Crystallogr.* **2009**, 42, 339–341.
- (61) Bain, G. A.; Berry, J. F. Diamagnetic Corrections and Pascal's Constants. *J. Chem. Educ.* **2008**, 85, 532.
- (62) Chilton, N. F.; Anderson, R. P.; Turner, L. D.; Soncini, A.; Murray, K. S. PHI: A powerful new program for the analysis of anisotropic monomeric and exchange-coupled polynuclear d- and f-block complexes. *J. Comput. Chem.* **2013**, 34, 1164–1175.
- (63) Edema, J. J. H.; Gambarotta, S.; Meetsma, A.; Van Bolhuis, F.; Spek, A. L.; Smeets, W. J. J. The unpredictable structural features of chromium(II) pyrrolys: synthesis and x-ray structures of monomeric square-planar (η^1 -2,5-Me₂C₄H₂N)₂Cr(py)₂, square-pyramidal (η^1 -C₄H₄N)₂Cr(py)₃, dimeric [(7-azaindolyl)₂Cr(DMF)]₂, and polymeric [(η^1 -2,5-Me₂C₄N₂)₄CrNa₂(THF)₂(Et₂O)]_n. An aborted Cr-Cr quadruple bond formation? *Inorg. Chem.* **1990**, 29, 2147–2153.
- (64) Edema, J. J. H.; Gambarotta, S.; Van Bolhuis, F.; Smeets, W. J. J.; Spek, A. L. New classes of monomeric and dimeric square-planar chromium(II) aryloxides: syntheses and structures. *Inorg. Chem.* **1989**, 28, 1407–1410.
- (65) Hermes, A. R.; Morris, R. J.; Girolami, G. S. Twelve-electron organochromium species: synthesis and characterization of high-spin square-planar chromium(II) alkyls and aryls. *Organometallics* **1988**, 7, 2372–2379.
- (66) Zhou, W.; Therrien, J. A.; Wence, D. L. K.; Yallits, E. N.; Conway, J. L.; Patrick, B. O.; Smith, K. M. Cyclopentadienyl mesityl complexes of chromium(II) and chromium(III). *Dalton Trans.* **2011**, 40, 337–339.
- (67) Wang, J.; Tan, G.; An, D.; Zhu, H.; Yang, Y. Organochromium(II) and Organonitridochromium(V) N-Heterocyclic Carbene Complexes: Synthesis and Structural Characterization. *Z. Anorg. Allg. Chem.* **2011**, 637, 1597–1601.
- (68) Voges, M. H.; Rømming, C.; Tilsted, M. Synthesis and Characterization of 14-Electron Cyclopentadienyl Chromium(II)

- Complexes Containing a Heterocyclic Carbene Ligand. *Organometallics* **1999**, *18*, 529–533.
- (69) van der Eide, E. F.; Helm, M. L.; Walter, E. D.; Bullock, R. M. Structural and Spectroscopic Characterization of 17- and 18-Electron Piano-Stool Complexes of Chromium. Thermochemical Analyses of Weak Cr–H Bonds. *Inorg. Chem.* **2013**, *52*, 1591–1603.
- (70) Simler, T.; Danopoulos, A. A.; Braunstein, P. N-Heterocyclic carbene-phosphino-picolines as precursors of anionic 'pincer' ligands with dearomatized pyridine backbones; transmetallation from potassium to chromium. *Chem. Commun.* **2015**, *51*, 10699–10702.
- (71) Pugh, D.; Wright, J. A.; Freeman, S.; Danopoulos, A. A. 'Pincer' dicarbene complexes of some early transition metals and uranium. *Dalton Trans.* **2006**, 775–782.
- (72) Kreisel, K. A.; Yap, G. P. A.; Theopold, K. H. A Chelating N-Heterocyclic Carbene Ligand in Organochromium Chemistry. *Organometallics* **2006**, *25*, 4670–4679.
- (73) Jones, C.; Dange, D.; Stasch, A. Synthesis and Crystal Structures of Two N-Heterocyclic Carbene Adducts of CrCl₂. *J. Chem. Crystallogr.* **2012**, *42*, 494–497.
- (74) Downing, S. P.; Guadaño, S. C.; Pugh, D.; Danopoulos, A. A.; Bellabarba, R. M.; Hanton, M.; Smith, D.; Tooze, R. P. Indenyl- and Fluorenyl-Functionalized N-Heterocyclic Carbene Complexes of Titanium, Zirconium, Vanadium, Chromium, and Yttrium. *Organometallics* **2007**, *26*, 3762–3770.
- (75) Danopoulos, A. A.; Monakhov, K. Y.; Robert, V.; Braunstein, P.; Pattacini, R.; Conde-Guadano, S.; Hanton, M.; Tooze, R. P. Angular Distortions at Benzylic Carbons Due to Intramolecular Polarization-Induced Metal–Arene Interactions: A Case Study with Open-Shell Chromium(II) NHC Complexes. *Organometallics* **2013**, *32*, 1842–1850.
- (76) Conde-Guadano, S.; Danopoulos, A. A.; Pattacini, R.; Hanton, M.; Tooze, R. P. Indenyl Functionalized N-Heterocyclic Carbene Complexes of Chromium: Syntheses, Structures, and Reactivity Studies Relevant to Ethylene Oligomerization and Polymerization. *Organometallics* **2012**, *31*, 1643–1652.
- (77) Abernethy, C. D.; Clyburne, J. A. C.; Cowley, A. H.; Jones, R. A. Reactions of Transition-Metal Metallocenes with Stable Carbenes. *J. Am. Chem. Soc.* **1999**, *121*, 2329–2330.
- (78) Gross, Z. High-valent corrole metal complexes. *JBIC, J. Biol. Inorg. Chem.* **2001**, *6*, 733–738.
- (79) Lin, H. M.; Sheu, H. S.; Wang, C. C.; Che, C. M.; Wang, Y. Structural and electron density studies on a chromium(IV)-oxo complex Cr^{IV}(O)(TMP). *J. Chin. Chem. Soc.* **1999**, *46*, 487–493.
- (80) Monillas, W. H.; Yap, G. P. A.; Theopold, K. H. Reactivity of a low-valent chromium dinitrogen complex. *Inorg. Chim. Acta* **2011**, *369*, 103–119.
- (81) Lin, K. M.; Wang, P. Y.; Shieh, Y. J.; Chen, H. Z.; Kuo, T. S.; Tsai, Y. C. Reductive N–N bond cleavage and coupling of organic azides mediated by chromium(I) and vanadium(I) beta-diketiminato. *New J. Chem.* **2010**, *34*, 1737–1745.
- (82) Cowley, R. E.; Bill, E.; Neese, F.; Brennessel, W. W.; Holland, P. L. Iron(II) Complexes with Redox-Active Tetrazene (RNNNNR) Ligands. *Inorg. Chem.* **2009**, *48*, 4828–4836.
- (83) Barron, A. R.; Salt, J. E.; Wilkinson, G.; Motevalli, M.; Hursthouse, M. B. The Chemistry of chromium nitrile complexes of 1,2-bis(dimethylphosphino)-ethane - X-ray crystal structures of trans-Cr^{IV}Cl(NEt)(DMPE)₂ CF₃SO₃, trans-Cr^{IV}(N=CHMe)₂(DMPE)₂ BPh₄, and trans-Co⁰(NCMe)₂(DMPE)₂ BPh₄. *J. Chem. Soc., Dalton Trans.* **1987**, 2947–2954.
- (84) Moubarak, B.; Murray, K. S.; Nichols, P. J.; Thomson, S.; West, B. O. The synthesis, reactivity and magnetic susceptibilities of Cr(IV)porphyrin imido complexes, CrN(R), and attempts to form heterobinuclear μ -imido compounds with CrN(R)V and CrN(R)Fe bridges. *Polyhedron* **1994**, *13*, 485–495.
- (85) Labinger, J. A.; Bercaw, J. E. Understanding and exploiting C–H bond activation. *Nature* **2002**, *417*, 507–514.
- (86) Hartwig, J. F. Borylation and Silylation of C–H Bonds: A Platform for Diverse C–H Bond Functionalizations. *Acc. Chem. Res.* **2012**, *45*, 864–873.
- (87) Godula, K.; Sames, D. C–H bond functionalization in complex organic synthesis. *Science* **2006**, *312*, 67–72.
- (88) Jafarzadeh, M. Trimethylsilyl azide (TMSN₃): A versatile reagent in organic synthesis. *Synlett* **2007**, *2007*, 2144–2145.
- (89) Eikey, R. A.; Khan, S. I.; Abu-Omar, M. M. The Elusive Terminal Imido of Manganese(V). *Angew. Chem., Int. Ed.* **2002**, *41*, 3591–3595.
- (90) Goedkent, V. L.; Ercolani, C. Nitrido-bridged iron phthalocyanine dimers – synthesis and characterization. *J. Chem. Soc., Chem. Commun.* **1984**, 378–379.
- (91) Colomban, C.; Kudrik, E. V.; Tyurin, D. V.; Albrieux, F.; Nefedov, S. E.; Afanasiev, P.; Sorokin, A. B. Synthesis and characterization of μ -nitrido, μ -carbido and μ -oxo dimers of iron octapropylporphyrizine. *Dalton Trans.* **2015**, *44*, 2240–2251.
- (92) Niemann, A.; Bossek, U.; Haselhorst, G.; Wieghardt, K.; Nuber, B. Synthesis and Characterization of Six-Coordinate Nitrido Complexes of Vanadium(V), Chromium(V), and Manganese(V). Isolation of a Dinuclear, Mixed-Valent μ -Nitrido Chromium(III)/Chromium(V) Species. *Inorg. Chem.* **1996**, *35*, 906–915.
- (93) Verma, S.; Hanack, M. Synthesis of nitrido(phthalocyaninato)-metal(V) complexes RnPcMN (M = Re, Mo, W) and new compounds with nitrido-bridges between rhenium and elements of the third main group. *Z. Anorg. Allg. Chem.* **2003**, *629*, 880–892.
- (94) Studt, F.; Lamarche, V. M. E.; Clentsmith, G. K. B.; Cloke, F. G. N.; Tuzcek, F. Vibrational and electronic structure of the dinuclear bis(μ -nitrido) vanadium(V) complex V(N{N''})₂(μ -N)₂: spectroscopic properties of the M₂(μ -N)₂ diamond core. *Dalton Trans.* **2005**, 1052–1057.
- (95) Makarova, A. S.; Kudrik, E. V.; Makarov, S. V.; Koifman, O. I. Stability and catalytic properties of μ -oxo and μ -nitrido dimeric iron tetrasulphophthalocyanines in the oxidation of Orange II by tert-butylhydroperoxide. *J. Porphyrins Phthalocyanines* **2014**, *18*, 604–613.
- (96) Ansari, M.; Vyas, N.; Ansari, A.; Rajaraman, G. Oxidation of methane by an N-bridged high-valent diiron-oxo species: electronic structure implications on the reactivity. *Dalton Trans.* **2015**, *44*, 15232–15243.
- (97) Afanasiev, P.; Sorokin, A. B. μ -Nitrido Diiron Macrocyclic Platform: Particular Structure for Particular Catalysis. *Acc. Chem. Res.* **2016**, *49*, 583–593.
- (98) Odom, A. L.; Cummins, C. C. A Chromium(VI) Nitrido–Silylmethyl Complex and a Chromium(V) μ -Nitrido Dimer: Synthetic and Structural Details. *Organometallics* **1996**, *15*, 898–900.